Artif Life Robotics (2017) 22:391–397
DOI 10.1007/s10015-017-0370-5

ORIGINAL ARTICLE

Hardware neural network models of CPG and PWM for controlling servomotor system in quadruped robot

Mizuki Abe[1] · Kanji Iwama[1] · Minami Takato[1] · Ken Saito[1] · Fumio Uchikoba[1]

Received: 28 February 2017 / Accepted: 31 May 2017 / Published online: 22 June 2017

Abstract This paper discusses the pulse-type hardware neural networks (P-HNNs) that contain a central pattern generator (CPG) and a pulsewidth modulation (PWM) servomotor controller and the application to quadruped robots. The purpose of our study is mimicking the biological neural networks and reproducing the similar motion of the living organisms in the robot. The CPG of the living organism generates the walking rhythms. We mimicked this CPG by modeling the cell body and the synapse of the living organism. The developed CPG composed of the P-HNN output four pulse signal sequences and the four outputs are introduced to each leg of the quadruped robot. On the other hand, the angle of the servomotor is controlled by the PWM. The PWM is obtained by modeling the axon of the living organism. The CPG and the PWM servo control system perform the walking motion of the quadruped robot. Moreover, the gate pattern change of quadruped animals is reproduced by these P-HNNs.

This work was presented in part at the 22nd International Symposium on Artificial Life and Robotics, Beppu, Oita, January 19–21, 2017.

✉ Mizuki Abe
csmi16001@g.nihon-u.ac.jp

Minami Takato
takato@eme.cst.nihon-u.ac.jp

Ken Saito
kensaito@eme.cst.nihon-u.ac.jp

Fumio Uchikoba
uchikoba@eme.cst.nihon-u.ac.jp
http://www.eme.cst.nihon-u.ac.jp/~uchikoba/

[1] Nihon University, 7-24-1 Narashinodai, Funabashi-shi, Chiba 274-8501, Japan

Keywords Quadruped robot · Locomotion rhythm · Pulse-type hardware neural networks · Synchronization phenomena · Oscillatory patterns · PWM control

1 Introduction

Conventional robots are usually controlled by digital processors and software programs. The digital software controlled robot has expanded to the various fields. However, the digital software control performs only a limited routine and it is very difficult to adapt unexpected events. A huge sized system is required if it treats whole possible cases. On the contrary, living organisms cope with even unexpected events. Thus, analysis and mimicking the living organism are quite interesting to achieve such adaptable and autonomous control systems.

Actual living organisms use neural networks and they are quite different from the digital system. From these viewpoints, many researches on the artificial neural networks (ANNs) have been conducted. Hodgkin–Huxley equations are examples of original study [1]. They analyzed the firing mechanism inside the cell of the neuron and presented four equations that describe the membrane potential and the ion flow. Studies of ANNs are roughly divided into two types: software models and hardware models. Software models are numeric value simulation methods by a computer calculation. In the large-scale neural networks using software models, it is difficult to process in continuous time, because the calculation speed and the amount are limited by the computer performance.

By contrast, hardware models such as FitzHugh–Nagumo model are different from software models [2]. It imitates the neural networks by analog electronic circuits. Sekine et al. improved the pulse-type hardware neural

network (P-HNN) model using lambda-shaped transistor [3]. This circuit composed of simple elements of transistors and resistors and capacitors. The relationship between the firing mechanism of the living organism and the circuit was addressed in this model. The nonlinear operation by the electronic circuit can perform at high speed and process in continuous time. Therefore, the neural networks can generate the output in real time even if the circuit scale becomes large.

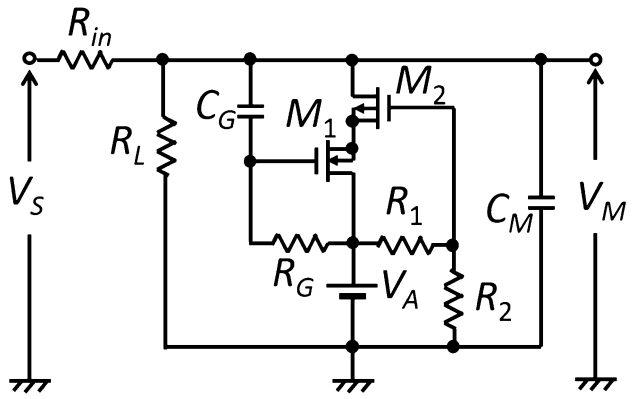

Fig. 1 Circuit diagram of the cell

The rhythm of walking motion of the living organism is generated by the CPG. The CPG is composed of biological neural networks. The CPG of the living organism includes the cell body and the synapse, and they are mutually connected. Analog and digital technologies are used for modeling and implementing the CPG as well as the ANNs. In digital technology, there is research using FPGA to overcome circuit scale and responsiveness [4]. However, from the viewpoint of reproducibility of biological CPG, the CPG model using pulse signals by analog circuits is considered to be useful. In our previous paper, the biological central pattern generator (CPG) was modeled by the P-HNNs for the robot controller [5]. In the CPG model, both the cell body and the synapse were modeled with

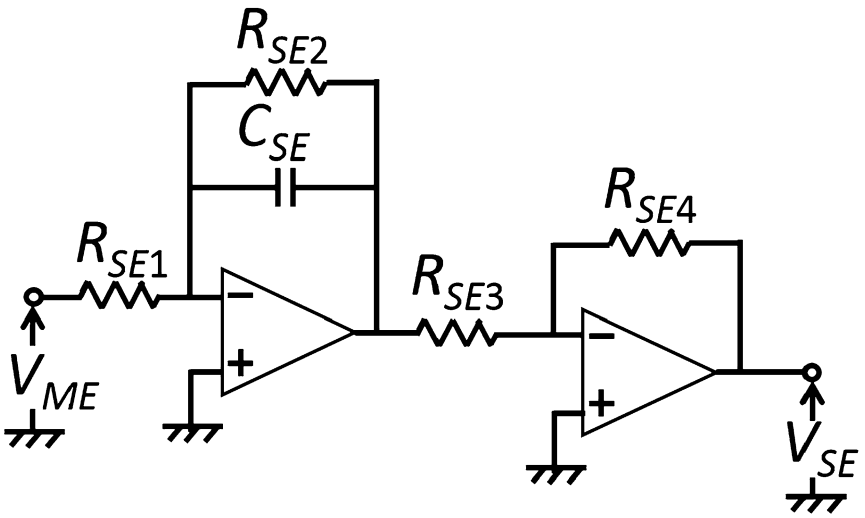

(a) Excitatory synaptic model

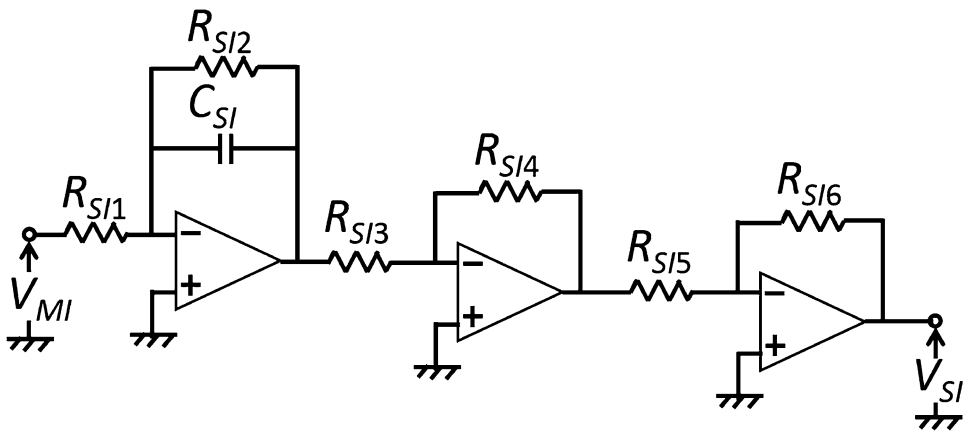

(b) Inhibitory synaptic model

Fig. 2 Circuit diagram of the synaptic model. **a** Excitatory synaptic model. **b** Inhibitory synaptic model

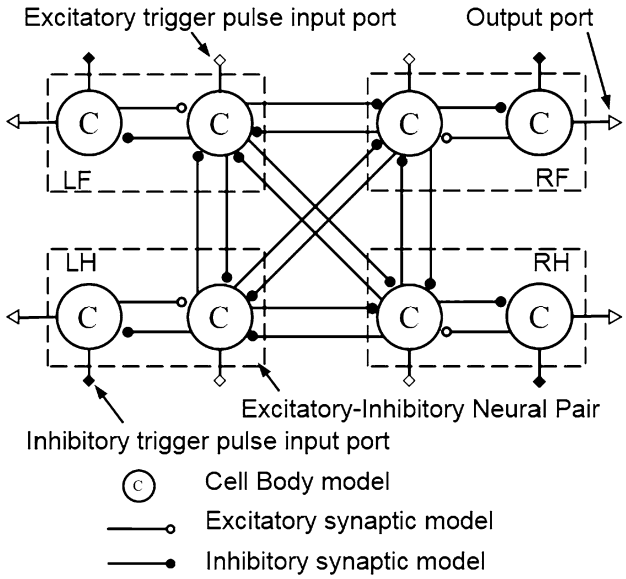

Fig. 3 CPG by the cell body model and the synaptic model

the analog electronic circuits. The lambda-shaped transistor was used in the cell body model. In addition, both the models of cell body and the synapse were integrated in CMOS IC and mounted on the millimeter size robot [5–7]. The PWM control system was also constructed by the P-HNNs. Modeling the axon of the living organism by the analog electronic circuit, the axon model was used for PWM [8].

Although the previous models of CPG and PWM were developed separately, in this paper, the function of the CPG was combined with PWM system. The CPG and the PWM servo control system achieve the walking control function of the quadruped robot by generating the walking rhythm and controlling the servo angle simultaneously. The four CPG outputs give the motion timing corresponded to each leg of the quadruped robot. On the other hand, PWM of axon models gives the servomotor angles of the four robot legs. This presented P-HNNs' system reproduces the gate pattern change of quadruped animals. There are very few examples, where the controller and the interface are integrated using only the P-HNNs and applied to the mechanical system. In this paper, we report as one of these few examples.

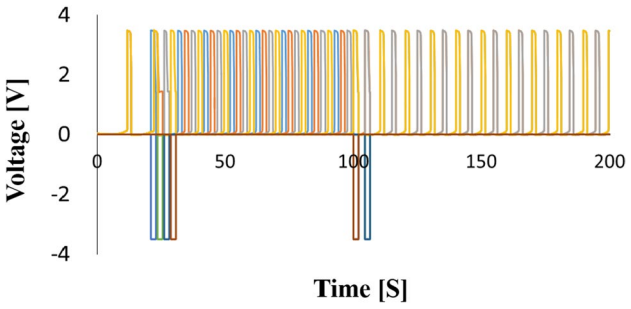

Fig. 5 Simulation of the locomotion rhythm (external trigger pulse as "Walk" and "Trot")

2 Pulse-type hardware neural networks

2.1 Cell body and synapse models

Figure 1 shows the circuit diagram of the cell body model. The cell body model was constructed based on models of Sekine using Λ-type transistor. The cell body model reproduces thresholds, refractory periods, action potentials, etc. which are features of neurons by the living organisms. The cell body model includes resistors R_1 and R_2, a membrane capacitor C_M, a voltage source V_A, a leak resistor R_L, a resistor R_G, and the capacitor C_G. The voltage control-type negative resistance circuit with an equivalent inductance is consisted of the n-channel MOSFET M_1 and the p-channel MOSFET M_2.

The negative resistance property enables the generation of a continuous action potential V_M by a selfexcited and also a separately-excited oscillation. Moreover, the cell body model can switch these oscillation types by changing V_A. When V_A is above the threshold, the separately-excited oscillation is generated by inputting the output voltage of synaptic model or the direct-current voltage stimulus to V_S. When V_A is removed, the input of V_S is output as a V_M including the time constant by R_L and C_M.

The circuit parameters of the cell body model for the CPG were as follows: $R_{in} = 330$ [kΩ], $R_L = 10$ [kΩ], $R_G = 680$ [kΩ], $R_1 = 20$ [kΩ], $R_2 = 15$[kΩ], $C_M = 470$ [nF], $C_G = 4.7$[μF], $V_A = 3.5$ [V], M_1: BSS83, and M_2: BHS205. The output pulse amplitude, the cycle time, and pulsewidth were 3.5 [V], 8 [s], and 1.6 [s], respectively.

Fig. 4 Relative phase difference of quadruped patterns compared with "Walk" and "Trot"

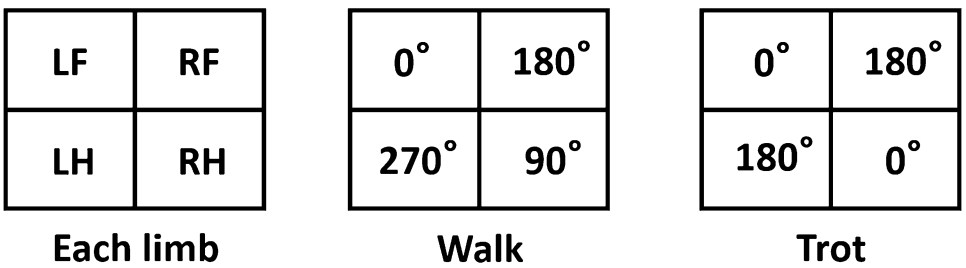

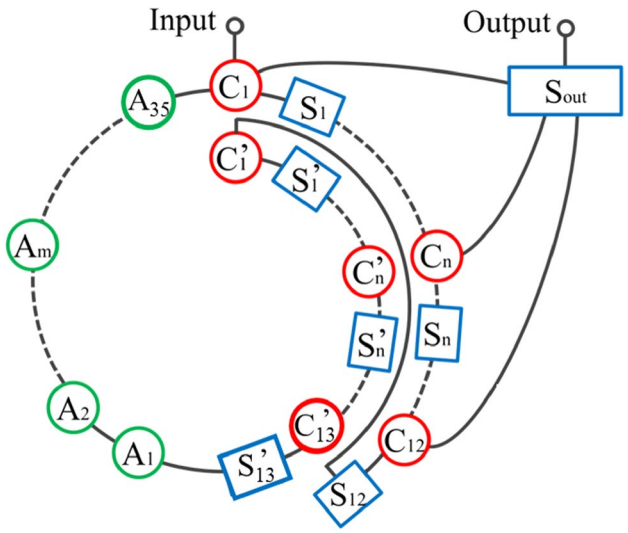

Fig. 6 Diagram of the PWM servo control system

Figure 2 shows the circuit diagram of the synaptic model. The synapses of the living organisms connect neurons and determine the influence of signals of excited neuron to the next neuron. The synapse can be divided into two types according to synapse coupling coefficient w of the element to determine influences. One is the excitatory synapse that enhances the excitement of the next neurons. The other is the inhibitory synapse that suppresses the excitation of the next neurons. Figure 2a shows the excitatory synaptic model and Fig. 2b shows the inhibitory synaptic model, respectively. The synaptic model has the spatio-temporal adding characteristics similar to those of the living organism. The synaptic model outputs the voltage V_S (V_{SE} or V_{SI}) by spatio-temporal summation of the output of cell body model V_M. The spatial summation characteristics are realized by the adder. Both the synaptic models are composed of the adders of operational amplifiers. The adder includes an inverting amplifier using an operational amplifier, and the amplification factor of the inverting amplifier varies according to synaptic weight w:

$$w_E = R_{SE4}/R_{SE3}, \tag{1}$$

$$w_I = R_{SI6}/R_{SI5}. \tag{2}$$

The temporal summation characteristics are realized by the RC integrator of the operational amplifier. The inhibitory synaptic model is obtained by reversing the output of the excitatory synaptic model. The circuit parameters of synaptic models were as follows: R_{SE1}, R_{SE2}, R_{SE3}, $R_{SE4} = 1$ [MΩ], $C_{SE} = 4.7$ [μF], R_{SI1}, R_{SI2}, R_{SI3}, R_{SI4}, R_{SI5}, R_{SI6}, $= 1$ [MΩ], and $C_{SI} = 4.7$ [μF].

3 Application to control system

3.1 CPG

The synchronization phenomena of the cell body model change depending on the type of the synaptic model. The cell body model connected by the excitatory synaptic model causes the in-phase synchronization. The cell body model connected by the inhibitory synaptic model causes the antiphase synchronization. In addition, synchronization phenomena do not occur when V_A in Fig. 1 is removed.

We construct the CPG using the cell body model, the excitatory synaptic model, and the inhibitory synaptic model. In Fig. 3, big open circles indicate the cell body model, small open circles indicate the excitatory synaptic model, and small solid circles indicate the inhibitory synaptic model, respectively. The CPG consisted of 8 cell body models, 4 excitatory synaptic models, and 16 inhibitory synaptic models.

Fig. 7 Circuit diagram of the synaptic model for PWM

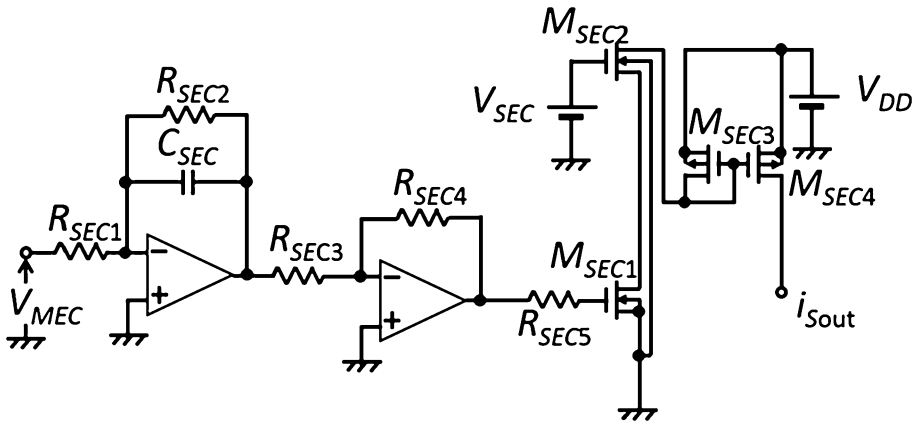

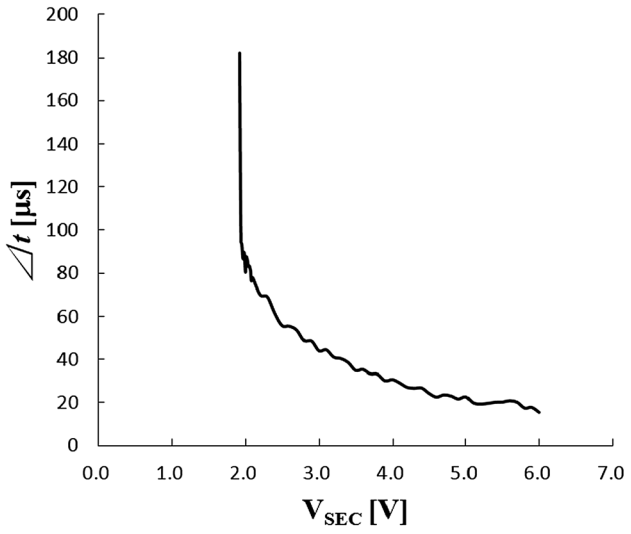

Fig. 8 Relationship between the time difference Δt and the synapse control voltage V_{SEC}

3.2 Walking rhythm generation by CPG

Four sets of excitatory–inhibitory-coupled cell body model generate the locomotion rhythms of legs (left fore limb, right fore limb, right hind limb, and left hind limb). When a trigger pulse is input to each cell body model, the walking rhythm changes.

Figure 4 shows the relative phase difference of quadruped patterns compared with "Walk" and "Trot". In this figure, each limb indicates left fore limb (LF), the right fore limb (RF), the right hind limb (RH), and the left hind limb (LH), respectively. In addition, the reference of the relative phase difference is LF (0 [°]). The quadruped locomotion patterns are regarded as different modes of coordination of the limb. Therefore, it is considered that quadruped locomotion pattern transitions arise from changing cooperation of the P-HNNs that control the interlimb coordination.

Figure 5 shows the simulation result of CPG model. In the first step, the trigger pulse of the "Walk" pattern was inputted to the cell body model. In the next step, the "Trot" pattern was inputted when the time reached to 100 [s]. In Fig. 5, the inhibitory trigger pulse is shown as negative pulses. By this process, the output pulse from four output ports of the CPG model corresponds to the pattern in Fig. 5.

3.3 PWM servo control system

What is important in this network is the tunable duty ratio and the constant cycle time. Figure 6 shows a circuit that can generate a PWM signal. C_1 to C_{12} (cell bodies) generate output pulses successively, and each pulsewidth is varied by the control voltage of S_1 to S_{12}. All sections from C_1 to C_{12} are connected to S_{out} (synapse). The total pulsewidth is generated by temporal adding the all the outputs of C_1 to C_{12} in S_{out}. In the section from C'_1 to S'_{13}, each cell body generates pulse in the same manner. However, the output is not connected to S_{out}. By adjusting the control voltage of S'_1 to S'_{13}, the constant cycle time is obtained. In the most case of the PWM, pulsewidth is much shorter than the cycle time. To obtain the long cycle time, the section from A_1 to A_{35} (axons) is used.

After a certain delay, the pulse signal returns to C_1. The pulsewidth can be adjusted by the control voltage of the synapse model. The axon model does not connect to S_{out}. The ring connection of the cell body, the synapse model, and the axon model generates continuous pulse trains. In the PWM servo control system, the number of cell body models was 25, the number of synaptic models was 25, and the number of axon models was 35 in total.

Using the P-HNNs model, the PWM control networks to control the servo motor were constructed. PWM servo motor (HRS-5498SG) was chosen from the commercial miniature robot motor. The cycle time was constant, and it was 16,040 [μs]. The actuation bound is −90 [°] to 90 [°], and total is 180°. The input pulse shows the minimum

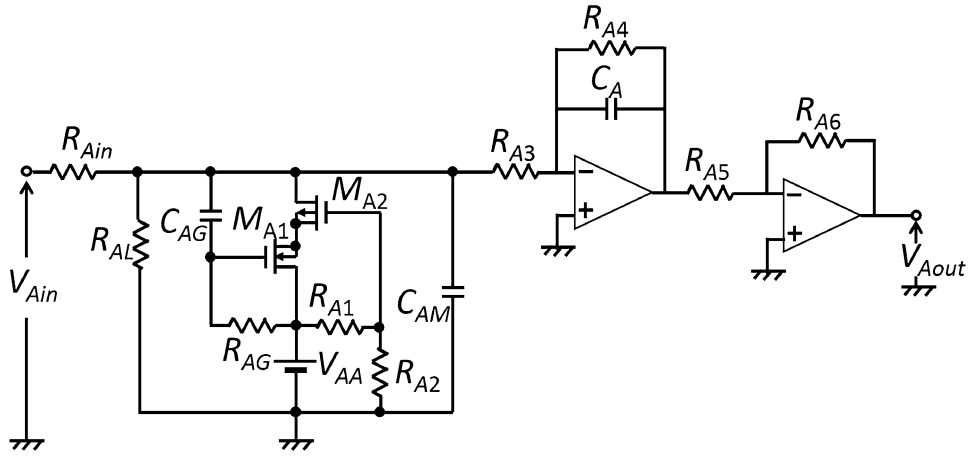

Fig. 9 Circuit diagram of the axon model

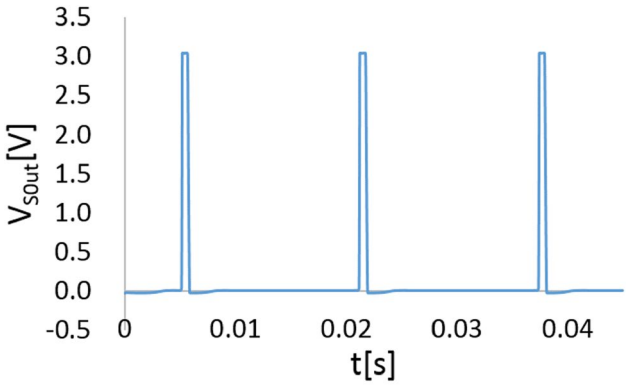

(a) Pulse width 600 [μs]

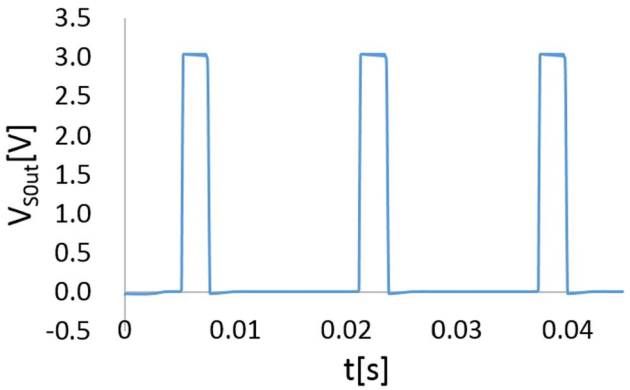

(b) Pulse width 2400 [μs]

Fig. 10 PWM output of S_{out}. **a** Pulsewidth 600 [μs]. **b** Pulsewidth 2400 [μs]

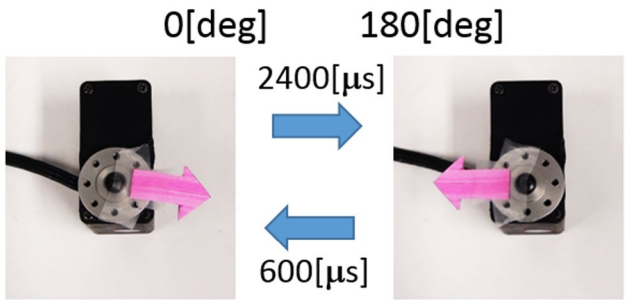

Fig. 11 Servo drive by P-HNNs

width as 600 [μs] when the objective degree is 0 [°], and when the objective degree is 180 [°], the input pulse shows the maximum width.

In the cell body model for the PWM servo control system, the parameters were as follows: $R_L = 10$ [kΩ], $R_G = 680$ [kΩ], $R_1 = 20$ [kΩ], $R_2 = 15$[kΩ], $C_M = 1.5$ [nF], $C_G = 1.2$ [μF], $V_A = 3.3$ [V], M_1: BSS83, and M_2: BHS205.

These circuit parameters were set as the cell body model could output the pulse amplitude 3.3 [V] and the pulsewidth 300 [μs] oscillating pulse. Figure 7 shows the circuit diagram of the synaptic model for PWM and it is corresponding to S_1 to S_{12} and S_1' to S_{13}. The excitatory synaptic model can adjust the synaptic coupling coefficient by the synapse control voltage V_{SEC}. It uses current i_{Sout} as output of the synapse and is connected with the current input of the cell body model. The excitatory synaptic model of the voltage control is obtained by adjusting the current amount of the current mirror composed of M_{SEC3} and M_{SEC4} with V_{SEC} connected to the gate terminal of M_{SEC2}. The circuit parameters of the synaptic models were as follows: R_{SEC1}, R_{SEC2}, R_{SEC3}, $R_{SE5} = 1$ [MΩ], $R_{SEC4} = 620$ [kΩ], $C_{SEC} = 1$ [pF], $V_{DD} = 5.0$ [V], M_{SEC1}, M_{SEC2}: BSS83, M_{SEC1}, and M_{SEC2}: BHS205.

The synapse coupling coefficient also rises due to the rise of V_{SEC}. When the signal of the cell body model on the input side of the synapse exceeds the threshold value of the cell body model on the output side, the higher the synaptic coupling coefficient, the smaller the time difference Δt of the pulse generation of the cell body model on the input side and the output side decreases. Figure 8 shows the relationship between the time difference Δt and the synapse control voltage V_{SEC} when the cell body model for the PWM system is connected to the input side and the output side.

Figure 9 shows the circuit diagram of the axon model. The axon model propagated a signal with a certain delay as those of living organisms. Delay characteristics of the axon model were obtained by the excitatory synaptic model and the cell body model. The circuit parameters of the axon model were as follows: $R_{Ain} = 100$ [kΩ], $R_{AL} = 10$ [kΩ], $R_{AG} = 680$ [kΩ], $R_{A1} = 20$ [kΩ], $R_{A2} = 15$ [kΩ], $C_{AM} = 1.5$ [nF], $C_{AG} = 1.2$ [μF], $V_{AA} = 3.3$ [V], M_{A1}: BSS83, M_{A2}: BHS205, R_{A3}, R_{A4}, R_{A5}, R_{A6}, $= 1$ [MΩ], and $C_A = 2.4$ [nF].

Figure 10 shows the output of S_{out} when the synapse control voltage V_{SEC} is adjusted. Figure 10a shows S_{out} when the pulsewidth is adjusted to 600 [μs]. Figure 10b shows when the pulsewidth is adjusted to 2400 [μs].

3.4 Evaluations of servo control system

A servo drive system was constructed by connecting one of the CPG output terminals and the PWM servo control system. Then, the result obtained by the simulation was written to FLUKE 284 Waveform Generator. FLUKE 284 can record and output simulation results in CSV file formats. Figure 11 shows photographs in which the servo motor is driven in the range of 0 [°] to 180 [°].

4 Conclusion

We discussed the CPG that can generate the walking pattern for the quadruped robot and the PWM control system that converts the signal to the PWM waveform. As a result, the constructed P-HNNs can output various gait patterns without using software programs. The PWM servo control system composed of P-HNNs was capable of generating PWM signals and control servo angle. P-HNNs generated walking pattern and servo angle simultaneously.

References

1. Hodgkin AL, Huxley AF (1952) A quantitative description of membrane current and its application to conduction and excitation in nerve. J Physiol 117:500–544
2. Nagumo J, Arimoto S, Yoshizawa S (1962) An active pulse transmission line simulating nerve axon. In: Proceedings of the IRE, pp 2061–2070
3. Sekine Y, Yamazaki A, Kurosawa H, Sato N (1995) Universal type hardware neuron model using lambdashaped transistor (in Japanese). IEICE Trans Inf Syst J78-D-2(1):131–139
4. Barron-Zambrano JH, Torres-Huitzil C, Girau B (2012) Configurable embedded CPG-based control for robot locomotion. Int J Adv Rob Syst 9:92
5. Saito K, Ikeda Y, Takato M, Sekine Y, Uchikoba F (2015) Development of quadruped robot with locomotion rhythm generator using pulse-type hardware neural networks. Artif Life Robot 20(4):366–371
6. Saito K, Saeki K, Sekine Y (2009) Synchronization of coupled pulse-type hardware neuron models for CPG model. In: Proceedings of the 2009 international joint conference on neural networks, Atlanta, Georgia, USA, pp 2748–2755
7. Iwata K, Okane Y, Ishihara Y et al (2016) Insect-type microrobot with mounted bare chip IC of artificial neural networks. In: Proceedings of the 29th IEEE international conference on micro electro mechanical systems, pp 1204–1207
8. Hara Y, Obara H, Uchikoba F, Saito K (2013) Generation of PWM waveform for servo motor using pulse-type hardware neural networks inspired by the brain of living organism (in Japanese). In: No. 13-2 proceedings of the 2013 JSME conference on robotics and mechatronics 1P1-B09